JOURNAL OF THE MECHANICAL BEHAVIOR OF BIOMEDICAL MATERIALS 60 (2016) 617–627

Available online at www.sciencedirect.com

ScienceDirect

www.elsevier.com/locate/jmbbm

Research Paper

Compressive, diametral tensile and biaxial flexural strength of cutting-edge calcium phosphate cements

Jun Luo[a,1], *Ingrid Ajaxon*[a,1], *Maria Pau Ginebra*[b], *Håkan Engqvist*[a], *Cecilia Persson*[a,*]

[a]*Materials in Medicine, Division of Applied Materials Sciences, Department of Engineering Sciences, Uppsala University, Box 534, 751 21 Uppsala, Sweden*

[b]*Research Centre in Biomedical Engineering, Biomaterials Division, Department of Materials Science and Metallurgy, Technical University of Catalonia (UPC), Av. Diagonal 647, E08028 Barcelona, Spain*

ARTICLE INFO

Article history:
Received 27 January 2016
Received in revised form
25 March 2016
Accepted 29 March 2016
Available online 2 April 2016

Keywords:
Calcium phosphate cement
Brushite
Apatite
Compressive strength
Tensile strength
Flexural strength

ABSTRACT

Calcium phosphate cements (CPCs) are widely used in bone repair. Currently there are two main types of CPCs, brushite and apatite. The aim of this project was to evaluate the mechanical properties of particularly promising experimental brushite and apatite formulations in comparison to commercially available brushite- and apatite-based cements (chronOS™ Inject and Norian® SRS®, respectively), and in particular evaluate the diametral tensile strength and biaxial flexural strength of these cements in both wet and dry conditions for the first time. The cements' porosity and their compressive, diametral tensile and biaxial flexural strength were tested in wet (or moist) and dry conditions. The surface morphology was characterized by scanning electron microscopy. Phase composition was assessed with X-ray diffraction. It was found that the novel experimental cements showed better mechanical properties than the commercially available cements, in all loading scenarios. The highest compressive strength (57.2±6.5 MPa before drying and 69.5±6.0 MPa after drying) was found for the experimental brushite cement. This cement also showed the highest wet diametral tensile strength (10.0±0.8 MPa) and wet biaxial flexural strength (30.7±1.8 MPa). It was also the cement that presented the lowest porosity (approx. 12%). The influence of water content was found to depend on cement type, with some cements showing higher mechanical properties after drying and some no difference after drying.

© 2016 The Authors. Published by Elsevier Ltd. This is an open access article under the CC BY-NC-ND license (http://creativecommons.org/licenses/by-nc-nd/4.0/).

*Correspondence to: Division of Applied Materials Science, Department of Engineering Sciences, The Ångström Laboratory, Uppsala University, Uppsala, Sweden.
E-mail address: cecilia.persson@angstrom.uu.se (C. Persson).
[1]These authors contributed equally to this work.

http://dx.doi.org/10.1016/j.jmbbm.2016.03.028
1751-6161/© 2016 The Authors. Published by Elsevier Ltd. This is an open access article under the CC BY-NC-ND license (http://creativecommons.org/licenses/by-nc-nd/4.0/).

1. Introduction

Calcium phosphate cements (CPCs) are clinically used as bone void fillers and as complements to hardware in fracture fixation (Larsson and Bauer, 2002). They are produced by mixing one or more calcium phosphate based powders with a liquid phase to form a paste that sets into a hard cement in a restricted period of time. Different types of CPCs can be obtained depending on the pH of the chemical reaction: when the pH is higher than 4.2, the end product is basic CPC, apatite (such as hydroxyapatite (HA), calcium-deficient hydroxyapatite (CDHA), carbonated apatite); and when the pH is lower than 4.2, the product is acidic CPC, brushite (dicalcium phosphate dihydrate, DCPD) or monetite (dicalcium phosphate anhydrous, DCPA). The precipitation kinetics of monetite are slower than brushite, so brushite is generally formed as the main product when pH is lower than 4.2 (Bohner, 2007 and 2000). A main, clinically relevant difference between brushite and apatite is the solubility. Brushite is metastable under physiological conditions, and could be resorbed faster than apatite (Vereecke and Lemaître, 1990; Gisep et al., 2003). However, transformation of brushite to apatite may occur *in vivo* (Bohner, 2007).

Since the first commercial CPC products were introduced two decades ago, many more have become available and have showed promising results in terms of bone regeneration, but some issues remain to be solved (Bohner et al., 2005; Bohner, 2010). Ideally, a bone substitute material should have mechanical properties similar to the host bone. The mechanical properties of CPCs are however generally poor compared to the surrounding bone, in loading scenarios other than compressive. In fact, CPCs are only approved for use in non-load bearing applications or are not used alone in load-bearing applications. Therefore, knowledge of the mechanical properties is important for decisions regarding possible use in certain, well-defined load-bearing scenarios. However, there is a general lack of knowledge on mechanical properties other than compressive strength (CS) for CPCs (Zhang et al., 2014). In particular, there is no data on the biaxial flexural properties of commercially available CPCs.

Apatite is the most investigated CPC type, as it has traditionally shown a higher mechanical strength than brushite. However, brushite cements have attracted an increasing interest as they have shown faster setting and resorption than apatite cements *in vivo* (Bohner et al., 2005). Also, brushite cements with a strength matching that of apatite cements have recently been reported (Unosson and Engqvist, 2014; Engstrand et al., 2014), with a maximum wet CS of 91.8 MPa after setting for 24 h. On the other hand, a fast setting apatite cement with good mechanical strength (wet CS around 40 MPa) has also been developed recently, where almost full strength could be achieved in 24 h (Ginebra et al., 2004).

The aim of this study was to evaluate and compare the mechanical properties of the above recently developed cutting-edge experimental CPCs, i.e. the strong brushite cement and the fast setting apatite cement, with two commercially available brushite and apatite based cements, chronOS™ Inject and Norian® SRS®, respectively. chronOS™ Inject is a brushite based bone mineral substitute with low mechanical strength, similar to the lower range of cancellous bone (Donaldson and Wright, 2011). Norian® SRS® is a fast-setting apatite bone mineral substitute. It forms a low crystalline order and a small grain size carbonated apatite similar to the mineral phase of bone in comparison to sintered HA (Yetkinler et al., 1999).

CPCs are exposed to body fluids *in vivo*. However, the mechanical properties of the cements are often determined experimentally using dry specimens (Koh et al., 2015; Ajaxon and Persson, 2016). The water-saturation state is however a significant factor which could affect the mechanical properties of CPCs (Zhang et al., 2014; Pittet and Lemaître, 2000). In this study, the compressive, diametral tensile and biaxial flexural strength of experimental and commercial CPCs were evaluated in wet (or moist) and dry conditions. The porosity – as assessed by the water evaporation method and helium pycnometry – as well as the morphology and phase composition – as assessed by scanning electron microscopy (SEM) and X-ray diffraction (XRD), respectively; were also evaluated and correlated to the mechanical properties.

2. Materials and methods

Two experimental cements, a brushite cement (Unosson and Engqvist, 2014) and an apatite cement (Ginebra et al., 2004) and two commercial cements (chronOS™ Inject and Norian® SRS®) were used in the study. chronOS™ Inject (Synthes GmbH, Switzerland) is a biphasic cement (β-TCP granules are embedded in a brushite matrix) (Bohner et al., 2003), and Norian® SRS® (Norian Corp., USA) is a carbonated apatite cement (Constantz et al., 1995). At the time of testing, the available Norian® SRS® had expired (expired January 2011, tested March 2015, no unexpired cements available from the supplier). Although XRD was performed to verify the composition, this can be considered a limitation of the study.

2.1. Cement preparation

Fig. 1 presents an overview of the experimental cement preparation methods.

The experimental brushite cement was prepared according to previous work (Unosson and Engqvist, 2014). A liquid-to-powder ratio of 0.22 mL/g was used in this process. The starting powder contained monocalcium phosphate monohydrate (MCPM, Scharlau, Sentmenat, Spain) and β-tricalcium phosphate (β-TCP, Sigma-Aldrich, St. Louis, MO, USA) in a 45:55 molar ratio, together with 1 wt% disodium dihydrogen pyrophosphate (SPP, Sigma-Aldrich, St. Louis, MO, USA) for control of the setting time. The particle size of MCPM was sieved to less than 75 μm. The liquid was an aqueous solution of 0.5 M citric acid (Acros Organics, New Jersey, USA). To prepare the cement paste, the starting powder and the liquid were mixed for 1 min in a Cap-Vibrator (Ivoclar Vivadent AG, Schaan, Liechtenstein) to allow for more efficient mixing of the two phases. Then the cement paste was filled into rubber moulds using a spatula in order to obtain a cylinder or a disc with the desired size (6 mm in diameter and 13 mm in height for compressive strength (CS) test, 8 mm in diameter and

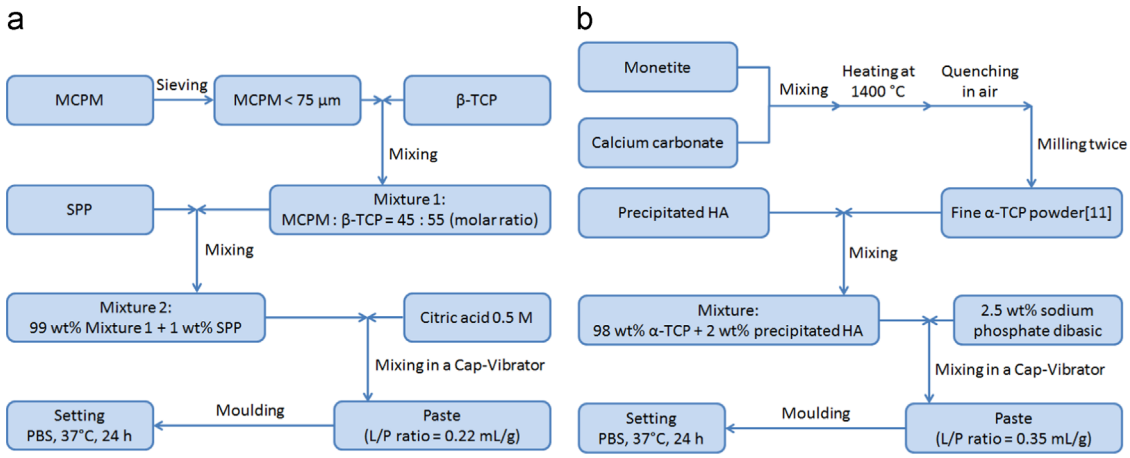

Fig. 1 – Schematic diagrams for the preparation methods of (a) experimental brushite and (b) experimental apatite.

3.5 mm in height for diametral tensile strength (DTS) test, 13 mm in diameter and 3 mm in height for biaxial flexural strength (BFS) test). After the cement specimens had set at room temperature (22±1 °C) for 5 min, they were immersed into phosphate buffered saline (PBS, Sigma-Aldrich, St. Louis, MO, USA, containing 0.01 M phosphate buffer, 0.0027 M potassium chloride and 0.137 M sodium chloride, pH 7.4) in sealed plastic containers and stored at 37 °C. The specimens were removed from the moulds after 24 h and prepared for subsequent tests.

For the experimental apatite cement, a liquid-to-powder ratio of 0.35 mL/g was used. The starting powder contained α-tricalcium phosphate (α-TCP) and 2 wt% of precipitated HA (Merck, Darmstadt, Germany) as a seed. The α-TCP powder was prepared by heating a mixture of monetite ($CaHPO_4$, Sigma Aldrich, St. Louis, MO, USA) and calcium carbonate ($CaCO_3$, Sigma Aldrich, St. Louis, MO, USA) at 1400 °C in a furnace (Hobersal, Caldes de Montbui, Spain). The samples were then quenched in air and milled twice in a planetary mill (Pulverisette 6, Fristsch GmbH, Idar-Oberstein, Germany) with an agate jar and balls to obtain a fine α-TCP powder (median particle size around 2 μm). The first milling sequence used 10 agate balls with a diameter of 30 mm at a speed of 450 rpm for 60 min. The second milling sequence used 100 agate balls with a diameter of 10 mm, using the same speed as the first sequence but for 70 min instead. The liquid used in the cement preparation was an aqueous solution consisting of 2.5 wt% sodium phosphate dibasic (Na_2HPO_4, Sigma Aldrich, St. Louis, MO, USA). The following cement specimen preparation was identical to the preparation of the experimental brushite cement.

The chronOS™ Inject had a liquid-to-powder ratio of 0.315 mL/g. According to the information from the manufacturer, the starting powder consisted of 42 wt% β-TCP, 31 wt% β-TCP granules with an average diameter smaller than 0.5 mm and a theoretical density close to 75% (Bohner et al., 2003), 21 wt% MCPM, 5 wt% magnesium hydrogen phosphate trihydrate and small amounts (<1 wt%) of sodium hydrogen pyrophosphate and magnesium sulfate (Apelt et al., 2004). The liquid consisted of a 0.5 wt% aqueous solution of sodium hyaluronate. The preparation process of the cement was identical to the experimental brushite cement except for the setting conditions of the cement. Since the chronOS™ Inject cement lacked sufficient cohesion to set to a solid in an aqueous solution, the specimens were, after they were left to set for 5 min in air at room temperature, placed in 100% relative humidity at 37 °C for 24 h to achieve moist specimens, rather than in PBS solution.

The Norian® SRS® had a liquid-to-powder ratio of 0.49 mL/g. According to the information from the manufacturer, the powder phase consisted of 85 wt% α-TCP, 12 wt% $CaCO_3$, and 3 wt% MCPM and a Na_2HPO_4 solution as the liquid phase. The cement preparation was the same as for the experimental cements.

2.2. *Mechanical testing*

The cement pastes were moulded in rubber moulds with 6 mm in diameter and 13 mm in height for CS tests. After the cements had set for 24 h, the obtained samples were polished using 800 grit SiC papers, in order to make the two ends flat and parallel and achieve a height of 12 mm according to the ASTM F451 standard for acrylic bone cements (ASTM, 2008). The samples for DTS tests were made in rubber moulds of 8 mm in diameter and 3.5 mm in height (Materials CoD, 1977). The samples were polished to a height of 3 mm after the cements had set for 24 h. Rubber moulds with 13 mm in diameter and 3 mm in height were used for BFS tests. The samples were polished after the cements had set for 24 h to obtain a thin circular disk of 2 mm thickness according to ASTM F 394-78 (ASTM, 1996). Some of the samples were placed for 24 h in a vacuum chamber (290 mbar) to dry them completely.

CS and DTS of samples before and after drying were measured using a universal testing machine (AGS-X, Shimadzu, Kyoto, Japan) at a cross-head speed of 1 mm/min until failure. A thin plastic film was positioned between the sample and the cross-head to distribute the load evenly. BFS was measured by a piston-on-3-ball test (ASTM Standard F394-78) (ASTM, 1996) in the same universal testing machine as the CS and DTS samples. Disc samples were centered and supported on three steel spheres with a diameter of 3.18 mm positioned 120° apart on a circle with a diameter of 10 mm. The entire test fixture was placed in the universal testing machine. A thin plastic film was placed between the sample

surface and the flat-ended piston (1.58 mm in diameter). Samples were tested at a cross-head speed of 1 mm/min until failure. The recorded fracture load was used to calculate the BFS using the following equation:

$$BFS = -0.2387P(X-Y)/d^2 \quad (1)$$

where P is the load at fracture (N); d is the thickness at the sample center (mm);

$$X = (1+\upsilon)\ln\left(\frac{B}{C}\right)^2 + \frac{1-\upsilon}{2}\left(\frac{B}{C}\right)^2 \quad (2)$$

$$Y = (1+\upsilon)\left[1+\ln\left(\frac{A}{C}\right)^2\right] + (1-\upsilon)\left(\frac{A}{C}\right)^2 \quad (3)$$

υ is Poisson's ratio; A is the radius of support circle (mm); B is the radius of loaded area (mm); and C is the sample radius (mm). For this study, a Poisson's ratio of 0.27 was used for all cement types (Dorozhkin, 2010).

For each type of mechanical test, ten or six samples per group were tested for experimental and commercially available cements, respectively.

2.3. Porosity

To calculate the porosity two different methods were used, water evaporation (Engstrand Unosson et al., 2015) and helium pycnometry. Helium pycnometry is a common method to measure the skeletal density of CPCs, afterwards, the porosity is calculated using the skeletal density and the apparent density that is obtained from Archimedes' principle. But the water evaporation method is less time consuming, it does not need any specific equipment and is cheaper when assessing the porosity of many specimens (Engstrand Unosson et al., 2015). Its validity for use with CPCs was hence further confirmed in the current study, by using both methods.

The apparent volume (V_a) of the samples was measured using Archimedes' principle in double distilled water at room temperature by utilizing a balance (NewClassic MF ML 104, Mettler Toledo AB, 0.1 mg, Greifensee, Switzerland) combined with a density kit (ML-DNY-43, Mettler-Toledo AB, Greifensee, Switzerland). After wet cements had been dried for 24 h in a vacuum chamber, the weight of the dry samples (m_d) was measured and the apparent density (ρ_a) was calculated according to

$$\rho_a = \frac{m_d}{V_a} \quad (4)$$

For the water evaporation method, the weight of 6 samples (6 mm in diameter, 12 mm in height) before drying was measured right after polishing. Water absorbed on the surface of the wet (or moist) samples was removed by moist Kimwipes® tissue paper before weighing. The water content in the samples was the difference between the weight before and after drying, afterwards, the volume of the evaporated water (V_w) was calculated from the division of the water content with the density of water. The porosity ($\varnothing_w$) measured by water evaporation was calculated according to

$$\varnothing_w(\%) = \left(\frac{V_w}{V_a}\right) \times 100 \quad (5)$$

For the helium pycnometry method, the skeletal density (ρ_s) of the samples was evaluated using helium pycnometry (AccuPyc 1340, Micromeritics, Norcross, GA, USA, maximum pressure of 19.5 Psi, chamber size of 1 cm^3) with 20 purges and 10 runs. Six samples (6 mm in diameter, 12 mm in height) of each CPC after drying were ground and homogenized before the measurement. The porosity ($\varnothing_h$) was calculated using the skeletal density and the apparent density (ρ_a) according to

$$\varnothing_h(\%) = \left(1-\frac{\rho_a}{\rho_s}\right) \times 100 \quad (6)$$

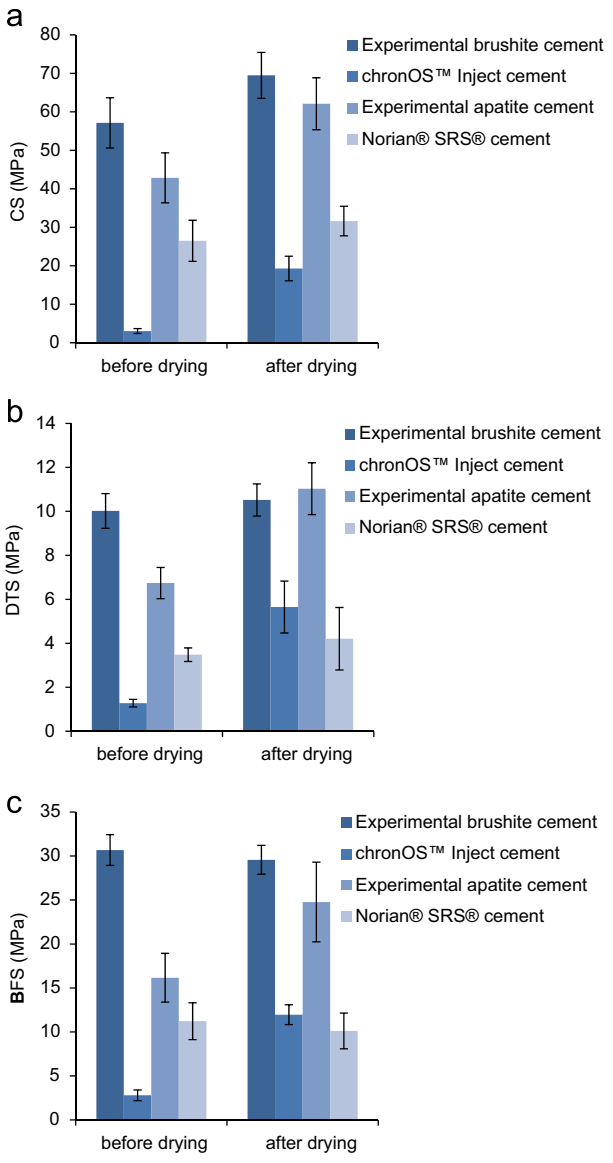

Fig. 2 – Mechanical properties of cements: (a) compressive strength (CS); (b) diametral tensile strength (DTS); and (c) biaxial flexural strength (BFS). The result presented is the average of between six to ten measurements per group. The error bars represent standard deviations of the mean.

2.4. Microstructure

The microstructure of fractured surfaces of dry samples was analyzed using scanning electron microscopy (SEM, LEO 1550,

Zeiss, Oberkochen, Germany) operated at an accelerating voltage of 6.00 kV. Three samples per group were evaluated with SEM. The samples were sputtered with a thin gold coating for 30 s before analysis. The scanning was performed at 6 kV with an in-lens detector.

2.5. Phase composition

To verify the phase composition, starting powders and hardened samples were analyzed with XRD. Samples from porosity measurements were thoroughly ground to a fine powder before XRD analysis. The XRD analysis was performed with a D8 Advance (Bruker AXS GmbH, Karlsruhe, Germany) in a theta–theta setup with Cu-Kα irradiation, nickel filter and using a beam knife. Diffraction patterns were collected between angles (2θ) of 5–60°, in steps of 0.02° with 0.25 s per step and using a rotation speed of 80 rpm. Quantitative phase composition analysis was done by Rietveld refinement with BGMN software (www.bgmn.de) (Taut et al., 1998; Bergmann et al., 1998) with Profex (http://profex.doebelin.org) (Doebelin and Kleeberg, 2015) as user interface. The reported result was the mean of three measurements with the repeatability taken as 2.77 × standard deviation according to ASTM E177-14 (ASTM, 2014). The structures used for the refinement were: β-TCP from PDF# 04-008-8714 (Dickens et al., 1974), β-calcium pyrophosphate (β-CPP) from PDF# 04-009-3876 (Boudin et al., 1993), monetite from PDF# 04-009-3755 (Dickens et al., 1971), MCPM from PDF# 04-011-3010 (Schroeder et al., 1975), brushite from PDF# 04-013-3344 (Curry and Jones, 1971), α-TCP from PDF# 04-010-4348 (Mathew et al., 1977), HA from PDF# 01-074-0565 (Sudarsanan and Young, 1969), calcite ($CaCO_3$) from PDF# 04-008-0788 (Maslen et al., 1993), newberyite ($MgHPO_4 \cdot 3H_2O$) from PDF# 04-010-2902 (Abbona et al., 1979), magnesium sulfate (β-$MgSO_4$) from PDF# 04-014-7920 (Weil, 2007).

2.6. Statistical analysis

IBM® SPSS® Statistics v. 22 (IBM Corp., Chicago, IL, USA) was used to analyze the variance (ANOVA). Scheffe's post-hoc test was then used to evaluate statistical differences between groups. Welch's robust test of equality of means and Tamhane's post-hoc test were used when homogeneity of variance could not be confirmed (using Levene's test). A significance level of $\alpha = 0.05$ was used in all above tests.

3. Results

3.1. Mechanical properties

The mechanical properties of cements before and after drying for 24 h in vacuum chamber are presented in Fig. 2. The wet CS was 57.2 ± 6.5 MPa for the experimental brushite cement, 3.0 ± 0.6 MPa for chronOS™ Inject cement, 42.9 ± 6.5 MPa for the experimental apatite cement and 26.5 ± 5.3 MPa for Norian® SRS® cement. As shown in Fig. 2a, the wet CS of the experimental brushite cement was about 19 times higher than chronOS™ Inject cement ($p < 0.001$). Additionally, the experimental apatite cement also had a significantly higher wet CS than Norian® SRS® cement ($p < 0.05$), although a smaller difference (1.6 times). After drying, the experimental cements were still significantly stronger than commercial cements ($p < 0.001$). The DTS and BFS of the four types of cements showed similar trends as the CS (Fig. 2b and c). The strength of chronOS™ Inject and the experimental apatite cement increased significantly after drying ($p < 0.05$). However, there was no statistically significant difference ($p > 0.05$) in any mechanical property for Norian® SRS® cement before and after drying. For the experimental brushite cement, only the CS showed a significant difference ($p < 0.05$) before and after drying.

3.2. Porosity

The porosity of the cements is shown in Table 1. The results for the two experimental cements calculated by the water evaporation method were similar to the values obtained by helium pycnometry ($p > 0.05$). The results for the commercially available cements were however statistically different ($p < 0.05$). The experimental brushite cement had the lowest porosity, at 11–12%, while the values of the other three cement types were all between 30% and 45%. However, the specimens of chronOS™ Inject cement were stored in 100% relative humid atmosphere, instead of aqueous solution, since pre-study specimens set in solution became too weak for normal handling. Therefore, not all pores could be considered water-filled for the porosity measurements of chronOS™ Inject using the water evaporation method, likely causing an error in the values. This is a limitation to the study.

3.3. Microstructure

The fractured surfaces' microstructures were assessed by SEM (Fig. 3). Many pores with sizes less than 30 μm in diameter appeared evenly distributed inside a homogeneous microstructure in the experimental brushite cement (Fig. 3a). This was in contrast to the chronOS™ Inject cement, which had some larger irregular pores with varying dimensions and some β-TCP granules with a size more than 100 μm in diameter, as illustrated by the white spheres embedded in the matrix in Fig. 3b. In the two apatite specimens (Fig. 3c and d), large pores were rarely found. The experimental apatite cement exhibited a similar microstructure to Norian® SRS® cement with a dense matrix and a regular microporous surface.

3.4. Phase composition

As shown in Fig. 4a and Fig. 5a, no unreacted MCPM was present in the experimental brushite cement while some β-CPP (7 ± 0.6 wt%) and β-TCP (7.4 ± 0.7 wt%) remained unreacted, and 81.8 ± 1.3 wt% brushite and 3.8 ± 0.4 wt% monetite appeared. The composition of the cement was similar to that found in a previous study (β-CPP: 5 wt%, β-TCP: 11 wt%, brushite: 78 wt%, monetite: 5 wt%) (Unosson and Engqvist, 2014). According to the XRD patterns (Fig. 4b) and the phase composition calculated from Rietveld refinement (Fig. 5b), the starting powder of chronOS™ Inject

Table 1 – Porosity of cements. Standard deviations are indicated within brackets.

Method	Experimental brushite cement	chronOS™ Inject	Experimental apatite cement	Norian® SRS®
Water evaporation	11.1% (0.9%)	33.3% (3.0%)	40.9% (1.0%)	43.8% (1.0%)
He pycnometry	12.1% (0.1%)	37.6% (0.4%)	41.7% (0.1%)	37.9% (0.2%)

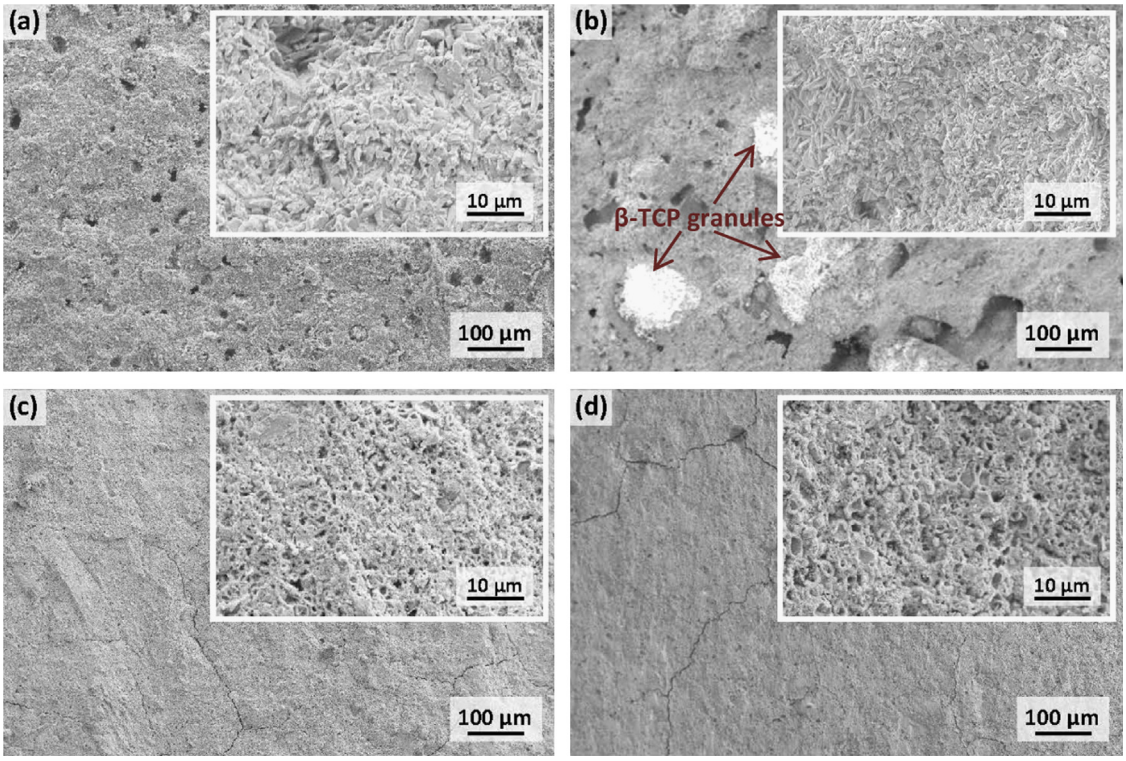

Fig. 3 – SEM micrographs of fractured surfaces of cements: (a) experimental brushite; (b) chronOS™ Inject; (c) experimental apatite; and (d) Norian® SRS®. Inserts are showing a higher magnification of a sample.

contained 71.1±0.7 wt% ß-TCP, 18.7±0.5 wt% MCPM, 6.2±0.2 wt% newberyite, 0.9±0.4 wt% magnesium sulfate and a small amount of monetite (3.1±0.3 wt%), to be compared to that stated by the manufacturer, i.e. β-TCP (73%), MCPM (21%), $MgHPO_4 \cdot 3H_2O$ (5%), $MgSO_4$ (<1%), $Na_2H_2P_2O_7$ (<1%) (Apelt et al., 2004). Magnesium sulfate, or any other phases containing $Mg^{2+}$and SO_4^{2-} groups, could not be detected in the set cement. The set cement of chronOS™ Inject contained 3.2±0.3 wt% newberyite, 7.2±1.1 wt% monetite, 34.4±3.9 wt% brushite and a large amount of unreacted ß-TCP (55.3±3.1 wt%). In the experimental apatite cement (Fig. 4c and Fig. 5c), more than 90% α-TCP reacted to form HA (91.4±2.5 wt%). The phase composition of Norian® SRS® starting powder showed less α-TCP (74.7±1.8 wt%) but more $CaCO_3$ (23.6±1.8 wt%) compared to the manufacturer's provided data (85 wt% α-TCP, 12 wt% $CaCO_3$, and 3 wt% MCPM) (Constantz et al., 1995) (Fig. 4d and Fig. 5d). However, a large amount of carbonated apatite (85.3±1.7 wt%) formed and about 5.3±1.3 wt% calcite remained unreacted in Norian® SRS® cement. The accuracy of the Rietveld refinement of the starting powders and set cements are shown in Figs. 6 and 7.

4. Discussion

In this study, two experimental CPCs and two commercial CPCs were evaluated in terms of their wet (or moist) and dry mechanical properties, porosity and microstructure.

Previously reported wet CS results (Unosson and Engqvist, 2014; Ginebra et al., 2004; Gisep et al., 2006) of the experimental brushite cement (about 70 MPa), chronOS™ Inject cement (about 4 MPa) and the experimental apatite cement (about 40 MPa) were similar to the results found in this study. While the CS for Norian® SRS® cement (26.5±5.3 MPa), was lower than the reported ultimate value (55 MPa) (Constantz et al., 1995), and lower than the value reported when prepared by a Rotary Mixer (46.6 MPa) (Jacobson, 2012), it was similar to the current study, when mixed by hand with a spatula (24.7 MPa) (Jacobson, 2012). The machine used (Cap-Vibrator) for mixing the powder with the liquid in this study might hence be less effective than the Rotary Mixer in achieving a homogeneous paste, with less air bubbles. Additionally, the phase composition of the starting powder of Norian® SRS® showed more $CaCO_3$ (23.6±1.8 wt%) than the manufacturer's provided data (12 wt% $CaCO_3$) (Constantz

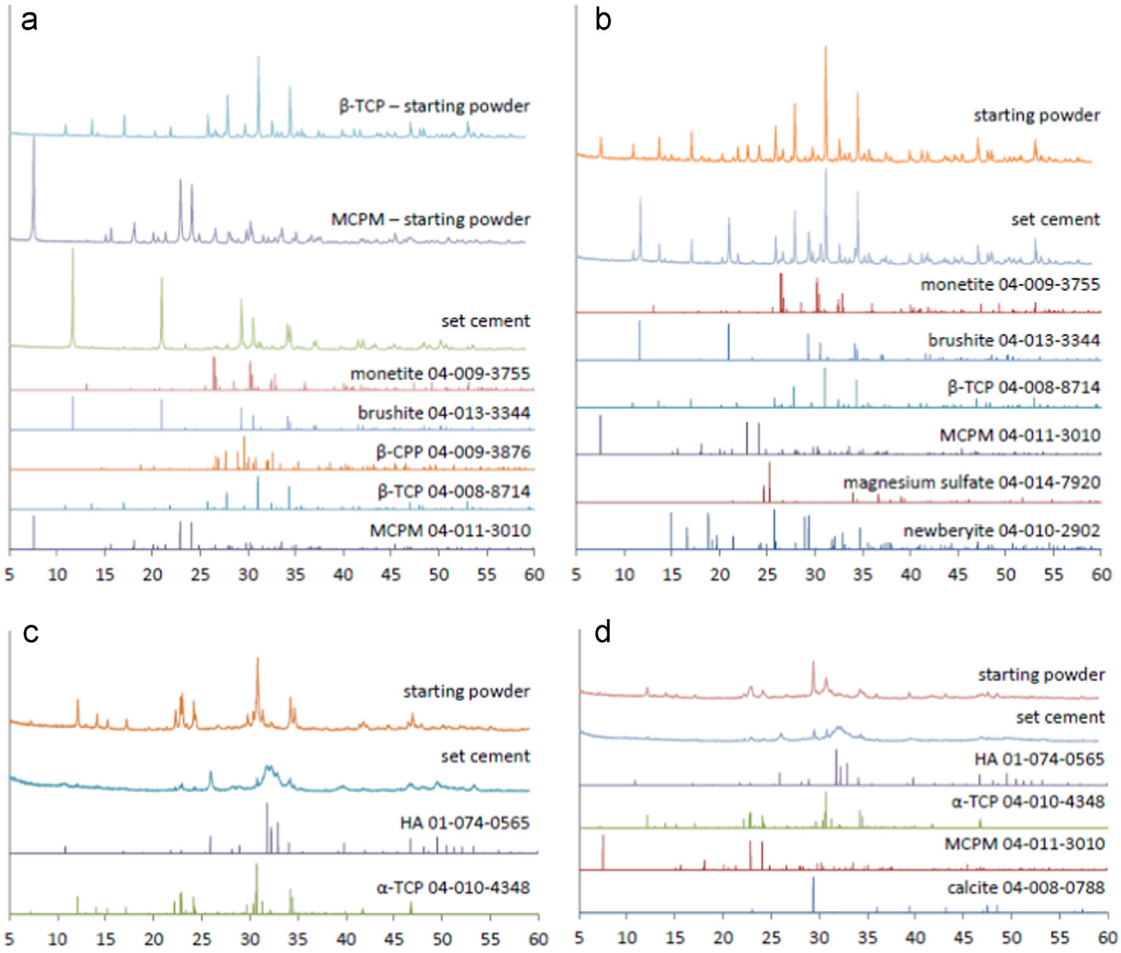

Fig. 4 – Representative XRD patterns of all compositions (one of three measurements is shown per composition) and the reference PDFs: (a) experimental brushite; (b) chronOS™ Inject; (c) experimental apatite; and (d) Norian® SRS®.

et al., 1995), and the cement had expired 50 months earlier. The CS of CPCs has previously been found to decrease with increased amounts of $CaCO_3$ (Sariibrahimoglu et al., 2012). However, no previous evaluation of the phase composition of Norian® SRS® could be found in the literature. Although the chronOS™ Inject showed a similar CS (3.0±0.6 MPa) to the previously reported value of 4 MPa, all the mechanical testing results for this cement were acquired from specimens stored in 100% relative humid atmosphere as opposed to truly wet specimens, having been immersed in an aqueous solution (storing them wet was not possible due to the low cohesion of the cement). These moist specimens presented a higher mechanical strength than wet specimens would have done, and is a limitation of the present study. However, similarly to the Norian® SRS® starting powder, the phase composition of chronOS™ Inject starting powder was slightly different to that reported by the manufacturer, with some monetite appearing in the starting powder, which decreased the reaction ratio and the mechanical strength of the set cement.

Due to their characteristic sensitivity to stress risers under tension, the compressive strength of CPCs is always higher than their tensile strength. Since it is difficult to measure the tensile strength of CPCs directly, indirect test methods have been used, such as DTS and BFS. The wet DTS of the experimental brushite cement (10.0±0.8 MPa) was very close to previously published data (10.2±0.8 MPa) (Unosson and Engqvist, 2014). The tensile strength (about 2.1 MPa) (Constantz et al., 1995) and flexural strength (about 0.5 MPa in 3-and 4-point bending) (Morgan DNY et al., 1997) have been reported for Norian® SRS® cement before. There are several methods to evaluate the flexural strength of ceramic materials, including piston-on-3-ball (BFS), 3-and 4-point bending (ASTM, 2003 and 2002; Ginebra et al., 2001). The piston-on-3-ball test is less sensitive to surface flaws than 3-and 4-point bending and tends to result in higher values than 3-point and 4-point bending (Morgan DNY et al., 1997). The authors could not identify any previous study on BFS for any of the four types of cements. However, DTS and BFS of other CPCs have been reported previously. Bermúdez et al. (1993) reported, in 1993, DTS tests of more than twenty types of CPCs developed around the world and found a maximum value of 2.8 MPa. Maenz et al. (2014) formed a brushite cement with 1.3±0.2 MPa in DTS and 6.9±0.8 MPa in BFS. An apatite cement with 10.2±1.7 MPa in DTS was formed by Takechi et al. (2004) by reaction of a mixture of tetracalcium phosphate and dicalcium phosphate anhydrous in 100% relative humidity.

The two experimental cements had better mechanical properties in all three types of mechanical tests than the two commercial cements. The experimental brushite

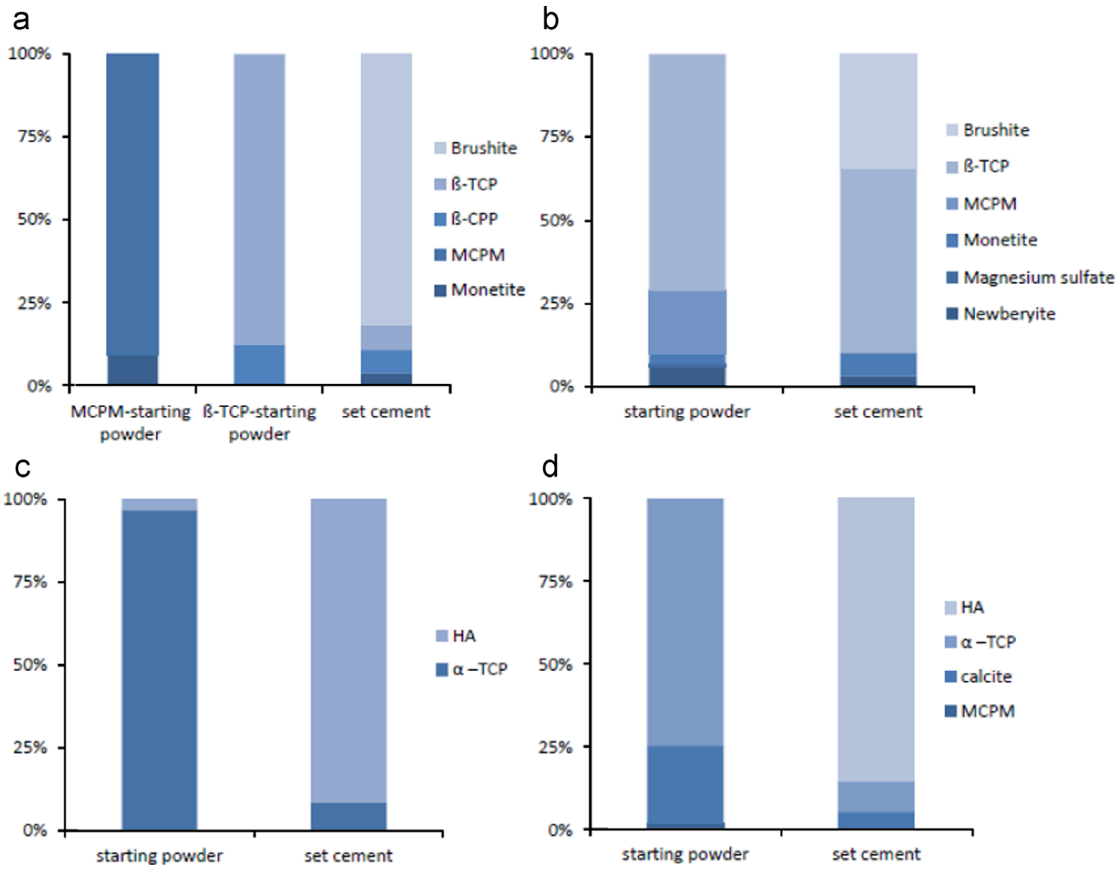

Fig. 5 – Phase composition of the starting powders and the set cements from XRD and Rietveld refinement: (a) the experimental brushite; (b) chronOS™ Inject; (c) the experimental apatite; and (d) Norian® SRS®. The relative errors for all groups were between 0.3 and 2.5 wt%.

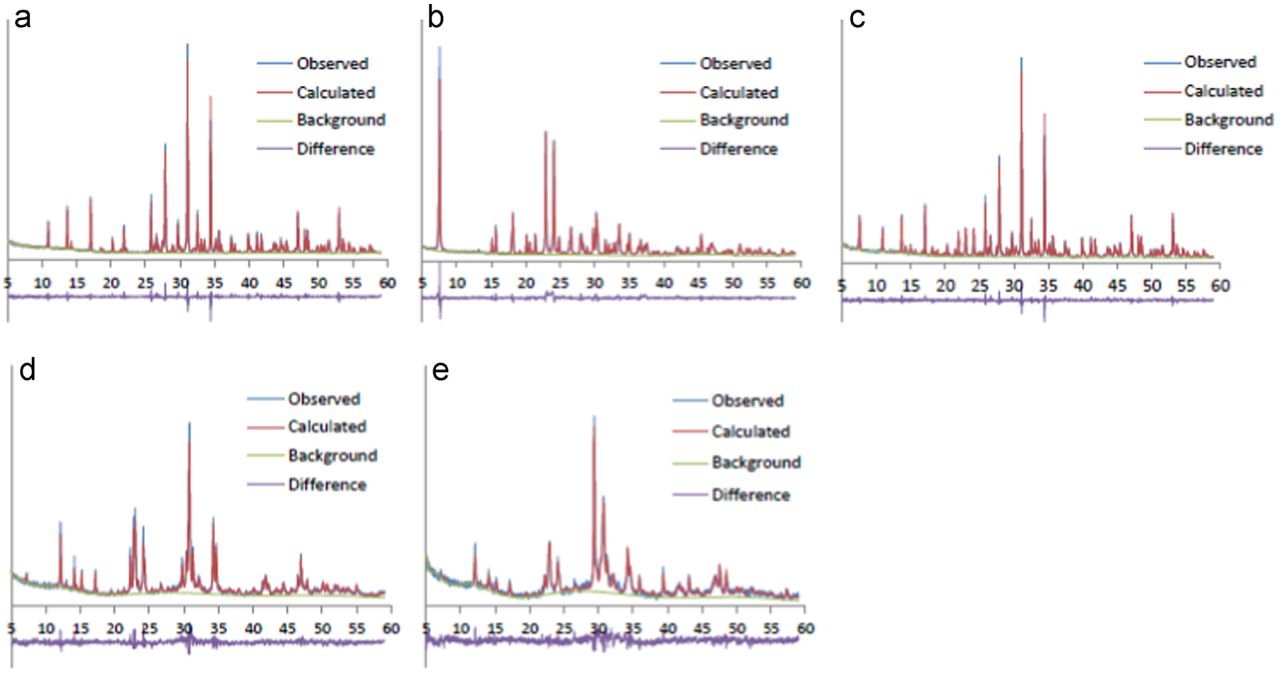

Fig. 6 – Starting powders of the Rietveld refinement accuracy as calculated by BGMN software: (a) MCPM – starting powder; (b) β-TCP – starting powder; (c) chronOS™ Inject – starting powder; (d) experimental apatite – starting powder; and (e) Norian® SRS®-starting powder.

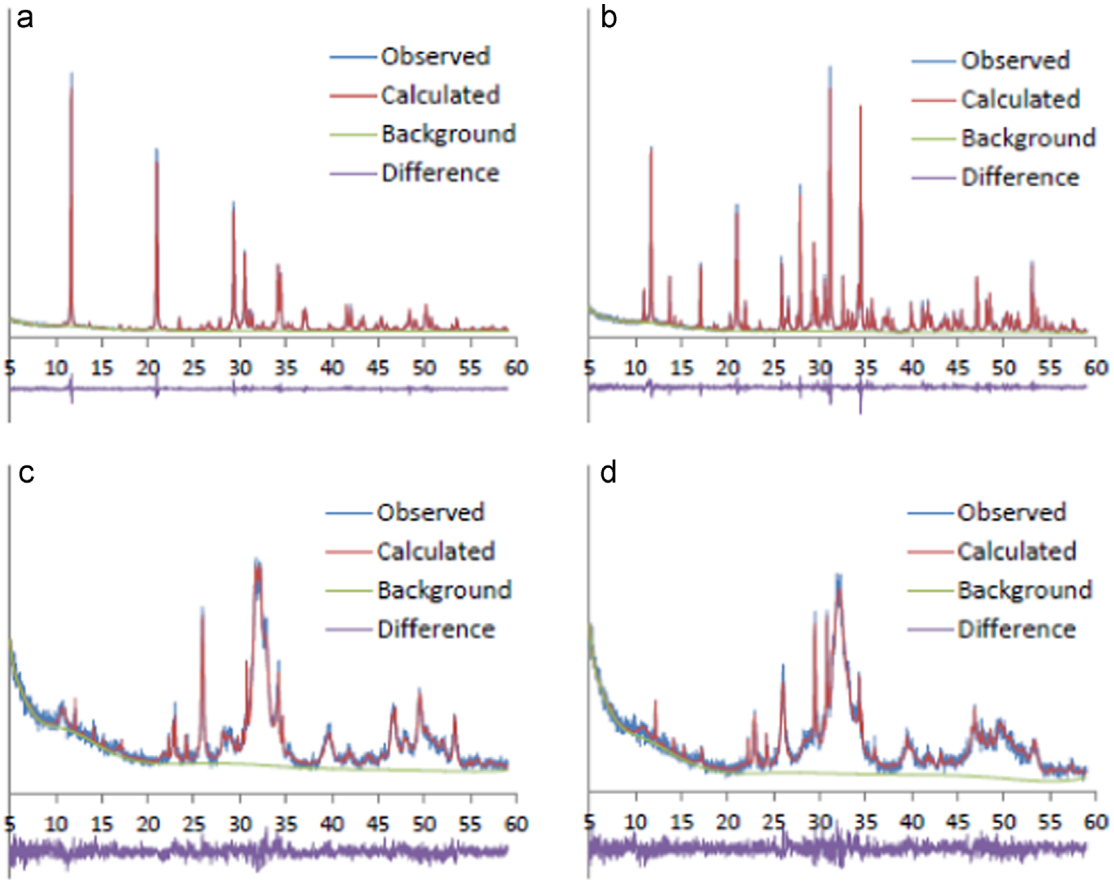

Fig. 7 – Cements of the Rietveld refinement accuracy as calculated by BGMN software: (a) experimental brushite cement; (b) chronOS™ Inject cement; (c) experimental apatite cement; and (d) Norian® SRS® cement.

cements showed significantly higher values than the other cements in the three types of mechanical tests when the specimens were tested before drying ($p<0.05$). However, there was no significant difference between the strengths of two experimental cements after drying ($p>0.05$). During setting of the brushite cement, the citric acid in the solution can reduce the pH value, increase the solubility of the starting powder and hence lead to a higher conversion into brushite (Fig. 5a). Hence, the crystal size and microstructure of the brushite become more homogeneous (Fig. 3a) after hardening, which could be beneficial to the mechanical properties of the cement. The citric acid also permits the usage of a lower L/P ratio, which contributes to the low porosity (Table 1), which is very beneficial for the mechanical strength. As shown in Fig. 3b, the chronOS™ Inject cement was biphasic and consisted of large granules of β-TCP (white spheres) in a matrix, and large uneven pores caused a high porosity which might be the main reasons for the poor mechanical properties of this type of cement.

Even though the porosity of the experimental apatite cement resembled that of the Norian® SRS® cement (Table 1), the mechanical strength of Norian® SRS® cement was significantly lower than the experimental apatite cement ($p<0.05$). As shown in Fig. 3c, small crystals filled most of the space in the experimental apatite cement. Small fractions of cavities between crystals and unreacted α-TCP particles, which would increase the porosity (Table 1) and weaken the cement, appeared. However, in agreement with previous studies (Ginebra et al., 2004), due to the high specific surface area of the starting powder and the small particle size, the fast setting to form HA and the high conversion rate (more than 90%) to HA (Fig. 5c) resulted in a compact network and a higher mechanical strength. Additionally, the composition of Norian® SRS® starting powder in this study (Fig. 5d) was different to the information obtained from the manufacturer, which may have affected the mechanical properties of cement. Moreover, some $CaCO_3$ was still unreacted after setting.

Ceramic bone cements are generally indicated as bone void fillers and are contra-indicated for load-bearing applications. However, if mechanical properties similar to the surrounding bone could be achieved, they could be adequate for use in certain, well-defined cases. The compressive strength and tensile strength (as measured in a uniaxial tensile test) of human trabecular bone has been reported to lie between 0.1–14 MPa and 1.3–3.5 MPa, respectively (Nazarian et al., 2008; Kopperdahl and Keaveny, 1998). This suggests that the experimental cements, presenting values at least the double of these in the wet condition, have the potential for use in certain load-bearing situations. Norian® SRS® also showed a higher compressive strength than trabecular bone, but its DTS was similar to the maximum tensile strength of bone. This latter one was measured in a uniaxial tensile test, which tends to give lower values than a DTS test,

suggesting that the tensile strength of Norian® SRS® may not reach that of trabecular bone. Again, using an optimal mixing method could have changed this conclusion. Finally, the mechanical properties of chronOS™ Inject, being in the lower range of trabecular bone, would severely restrict its possibilities for use in any load-bearing application.

Mechanical properties of dry CPCs have previously been reported to be higher than for wet specimens in similar conditions (Zhang et al., 2014; Pittet and Lemaître, 2000; Barralet et al., 2003). As shown in Fig. 2, the mechanical strength for some CPCs increased after drying, but not for Norian® SRS® cement. Also, only chronOS™ Inject cement and the experimental apatite cement showed statistically significant differences for the three types of mechanical properties before and after drying. For chronOS™ Inject cement, the increase was especially prominent, with all three types of mechanical properties after drying increasing with a factor of at least 4. Interestingly, there was no statistically significant difference ($p > 0.05$) for any of the three mechanical properties of Norian® SRS® cements before and after drying. Whereas this suggests that previously reported data for the dry mechanical properties of Norian® SRS® could potentially also be used as an approximate representation of the wet properties of the cement, it is not clear whether or not this similarity would be of importance to the clinical application, where the cement is always in a wet environment once implanted.

5. Conclusions

In this study, it was found that novel, high-strength experimental brushite cement and a fast setting experimental apatite cement showed higher CS, DTS and BFS than two commercially available cements (chronOS™ Inject, brushite based, and Norian® SRS®, apatite based), and also higher strengths than human trabecular bone. The experimental brushite cement displayed a consistently high strength and the lowest porosity among the cements. Dry CPCs have previously been found to display a higher strength than wet (or moist) CPCs under the same loading conditions. While this was indeed the case for chronOS™ Inject and the experimental cements, none of the three mechanical test results of Norian® SRS® cement changed significantly after drying. The results of this study support further development of the experimental CPCs towards clinical application.

Acknowledgments

The authors are grateful to the Swedish Foundation for International Cooperation in Research and Higher Education (STINT, Project IG2011-2047) and the Swedish Research Council (VR, Project 621-2011-6258) for funding. Montserrat Espanol and Yassine Maazouz in Technical University of Catalonia (UPC), Barcelona, Spain, are gratefully acknowledged for offering the starting powder for the experimental apatite cement. We also appreciate the support from the China Scholarship Council (CSC).

REFERENCES

Ajaxon, I., Persson, C., 2016. Mechanical properties of brushite calcium phosphate cements. In: Shi, D., Cheng, Y., Huang, J., Liu, Y., Zhang, B., Chang, J. (Eds.), The World Scientific Encyclopedia of Nanomedicine and Bioengineering I. World Scientific, Singapore.

Apelt, D., Theiss, F., El-Warrak, A.O., Zlinszky, K., Bettschart-Wolfisberger, R., Bohner, M., et al., 2004. *In vivo* behavior of three different injectable hydraulic calcium phosphate cements. Biomaterials 25, 1439–1451.

ASTM. ASTM F 451-08: Standard Specification for Acrylic Bone Cement, 2008.

ASTM. ASTM F 394-78: Standard Test Method for Biaxial Flexure Strength (Modulus of Rupture) of Ceramic Substrates, 1996.

ASTM. ASTM E 177-14: Standard Practise for Use of the Terms Precision and Bias in ASTM Test Methods, 2014.

Abbona, F., Boistelle, R., Haser, R., 1979. Hydrogen bonding in $MgHPO_4 \cdot 3H_2O$ (newberyite). Acta Crystallogr. Sect. B: Struct. Crystallogr. Cryst. Chem. 35, 2514–2518.

ASTM. ASTM D 790-03: Standard Test Methods for Flexural Properties of Unreinforced and Reinforced Plastic and Electrical Insulating Materials, 2003.

ASTM. ASTM D 6272-02: Standard Test Method for lexural properties–>Flexural Properties of Unreinforced and Reinforced Plastics and Electrical Insulating Materials by Four-Point Bending, 2002.

Bohner, M., 2007. Reactivity of calcium phosphate cements. J. Mater. Chem. 17, 3980–3986.

Bohner, M., 2000. Calcium orthophosphates in medicine from ceramics to calcium phosphate cements. Injury 31 (Suppl. 4), D37–D47.

Bohner, M., Gbureck, U., Barralet, J.E., 2005. Technological issues for the development of more efficient calcium phosphate bone cements: a critical assessment. Biomaterials 26, 6423–6429.

Bohner, M., 2010. Design of ceramic-based cements and putties for bone graft substitution. Eur. Cells Mater. 20, 3–10.

Bohner, M., Theiss, F., Apelt, D., Hirsiger, W., Houriet, R., Rizzoli, G., et al., 2003. Compositional changes of a dicalcium phosphate dihydrate cement after implantation in sheep. Biomaterials 24, 3463–3474.

Bergmann, J., Friedel, P., Kleeberg, R., 1998. BGMN—a new fundamental parameters based Rietveld program for laboratory X-ray sources, its use in quantitative analysis and structure investigations. CPD Newsl. 20, 5–8.

Boudin, S., Grandin, A., Borel, M.M., Leclaire, A., Raveau, B., 1993. Redetermination of the β-$Ca_2P_2O_7$ structure. Acta Crystallogr. Sect. C: Cryst. Struct. Commun. 49, 2062–2064.

Bermúdez, O., Boltong, M.G., Driessens, F.C.M., Planell, J.A., 1993. Compressive strength and diametral tensile strength of some calcium-orthophosphate cements: a pilot study. J. Mater. Sci.: Mater. Med. 4, 389–393.

Barralet, J.E., Hofmann, M., Grover, L.M., Gbureck, U., 2003. High-strength apatitic cement by modification with α-hydroxy acid salts. Adv. Mater. 15, 2091–2094.

Constantz, B.R., Ison, I.C., Fulmer, M.T., Poser, R.D., Smith, S.T., VanWagoner, M., et al., 1995. Skeletal repair by *in situ* formation of the mineral phase of bone. Science 267, 1796–1799.

Curry, N.A., Jones, D.W., 1971. Crystal structure of brushite, calcium hydrogen orthophosphate dihydrate: a neutron-diffraction investigation. J. Chem. Soc. A: Inorg. Phys. Theor., 3725–3729.

Donaldson, S., Wright, J.G., 2011. Recent developments in treatment for simple bone cysts. Curr. Opin. Pediatr. 23, 73–77.

Dorozhkin, S.V., 2010. Calcium orthophosphates as bioceramics: state of the art. J Funct. Biomater. 1, 22–107.

Doebelin, N., Kleeberg, R., 2015. Profex: a graphical user interface for the Rietveld refinement program BGMN. J. Appl. Crystallogr. 48, 1573–1580.
Dickens, B., Schroeder, L.W., Brown, W.E., 1974. Crystallographic studies of the role of Mg as a stabilizing impurity in β-$Ca_3(PO_4)_2$. The crystal structure of pure β-$Ca_3(PO4)_2$. J. Solid State Chem. 10, 232–248.
Dickens, B., Bowen, J.S., Brown, W.E., 1972. A refinement of crystal-structure of $CaHPO_4$ (synthetic monetite). Acta Crystallogr. Sect. B: Struct. Crystallogr. Cryst. Chem. 28, 797–806.
Engstrand, J., Persson, C., Engqvist, H., 2014. The effect of composition on mechanical properties of brushite cements. J. Mech. Behav. Biomed. Mater. 29, 81–90.
Engstrand Unosson, J., Persson, C., Engqvist, H., 2015. An evaluation of methods to determine the porosity of calcium phosphate cements. J. Biomed. Mater. Res. B: Appl. Biomater. 103, 62–71.
Gisep, A., Wieling, R., Bohner, M., Matter, S., Schneider, E., Rahn, B., 2003. Resorption patterns of calcium-phosphate cements in bone. J. Biomed. Mater. Res. Part A 66, 532–540.
Ginebra, M.P., Driessens, F.C., Planell, J.A., 2004. Effect of the particle size on the micro and nanostructural features of a calcium phosphate cement: a kinetic analysis. Biomaterials 25, 3453–3462.
Gisep, A., Curtis, R., Hanni, M., Suhm, N., 2006. Augmentation of implant purchase with bone cements: an *in vitro* study of injectability and dough distribution. J. Biomed. Mater. Res. B: Appl. Biomater. 77, 114–119.
Ginebra, M.P., Rilliard, A., Fernández, E., Elvira, C., San Román, J., Planell, J.A., 2001. Mechanical and rheological improvement of a calcium phosphate cement by the addition of a polymeric drug. J. Biomed. Mater. Res. 57, 113–118.
E. Jacobson, Norian Drillable: A Competitive Analysis, Synthes, Inc. or its affiliates, 2012.
Koh, I., López, A., Pinar, A.B., Helgason, B., Ferguson, S.J., 2015. The effect of water on the mechanical properties of soluble and insoluble ceramic cements. J. Mech. Behav. Biomed. Mater. 51, 50–60.
Kopperdahl, D.L., Keaveny, T.M., 1998. Yield strain behavior of trabecular bone. J. Biomech. 31 (7), 601–608.
Larsson, S., Bauer, T.W., 2002. Use of injectable calcium phosphate cement for fracture fixation: a review. Clin. Orthop. Relat. Res. 395, 23–32.
Materials CoD Devices, 1977. New American dental association specification no. 27 for direct filling resins. J. Am. Dent. Assoc. 94, 1191–1194.
Mathew, M., Schroeder, L.W., Dickens, B., Brown, W.E., 1977. The crystal structure of α-$Ca_3(PO_4)_2$. Acta Crystallogr. Sect. B: Struct. Crystallogr. Cryst. Chem. 33, 1325–1333.
Maslen, E.N., Streltsov, V.A., Streltsova, N.R., 1993. X-ray study of the electron-density in calcite, $CaCO_3$. Acta Crystallogr. B 49, 636–641.
Morgan, E.F., Yetkinler, D.N., Constantz, B.R., Dauskardt, R.H., 1997. Mechanical properties of carbonated apatite bone mineral substitute: strength, fracture and fatigue behaviour. J. Mater. Sci.: Mater. Med. 8, 559–570.
Maenz, S., Kunisch, E., Mühlstädt, M., Böhm, A., Kopsch, V., Bossert, J., et al., 2014. Enhanced mechanical properties of a novel, injectable, fiber-reinforced brushite cement. J. Mech. Behav. Biomed. Mater. 39, 328–338.
Nazarian, A., von Stechow, D., Zurakowski, D., Muller, R., Snyder, B.D., 2008. Bone volume fraction explains the variation in strength and stiffness of cancellous bone affected by metastatic cancer and osteoporosis. Calcif. Tissue Int. 83, 368–379.
Pittet, C., Lemaître, J., 2000. Mechanical characterization of brushite cements: a Mohr circles' approach. J. Biomed. Mater. Res. 53, 769–780.
Schroeder, L.W., Prince, E., Dickens, B., 1975. Hydrogen bonding in $Ca(H_2PO_4)_2.H_2O$ as determined by neutron diffraction. Acta Crystallogr. Sect. B: Struct. Crystallogr. Cryst. Chem. 31, 9–12.
Sudarsanan, K.T., Young, R.A., 1969. Significant precision in crystal structure details. Holly Springs hydroxyapatite. Acta Crystallogr. Sect. B: Struct. Crystallogr. Cryst. Chem. 25, 1534–1543.
Sariibrahimoglu, K., Leeuwenburgh, S.C., Wolke, J.G., Yubao, L., Jansen, J.A., 2012. Effect of calcium carbonate on hardening, physicochemical properties, and *in vitro* degradation of injectable calcium phosphate cements. J. Biomed. Mater. Res. A 100, 712–719.
Taut, T., Kleeberg, R., Bergmann, J., 1998. Seifert software: the new Seifert Rietveld program BGMN and its application to quantitative phase analysis. Mater. Struct. 5, 57–66.
Takechi, M., Miyamoto, Y., Momota, Y., Yuasa, T., Tatehara, S., Nagayama, M., et al., 2004. Effects of various sterilization methods on the setting and mechanical properties of apatite cement. J. Biomed. Mater. Res. B 69, 58–63.
Unosson, J., Engqvist, H., 2014. Development of a resorbable calcium phosphate cement with load bearing capacity. Bioceram. Dev. Appl. 4 1000074.
Vereecke, G., Lemaître, J., 1990. Calculation of the solubility diagrams in the system $Ca(OH)_2$–H_3PO_4–KOH–HNO_3–CO_2–H_2O. J. Cryst. Growth 104, 820–832.
Weil, M., 2007. The high-temperature modification of magnesium sulfate (beta-$MgSO_4$) from single-crystal data. Acta Crystallogr. E 63 i172-i172.
Yetkinler, D.N., Ladd, A.L., Poser, R.D., Constantz, B.R., Carter, D., 1999. Biomechanical evaluation of fixation of intra-articular fractures of the distal part of the radius in cadavera: Kirschner wires compared with calcium-phosphate bone cement. J. Bone Jt. Surg. Am. 81, 391–399.
Zhang, J., Liu, W., Schnitzler, V., Tancret, F., Bouler, J.M., 2014. Calcium phosphate cements for bone substitution: chemistry, handling and mechanical properties. Acta Biomater. 10, 1035–1049.